In this view, NVT is driven by conformational changes in the ground state; Figure 1 depicts the triplet energy along the ground-state trajectory and is not intended to show a mandatory path for relaxation in the isolated triplet. That it recognizes the necessity for considering modes of relaxation other than double-bond torsion is in our view an improvement over most previous energy profiles for arylalkene triplets.

Acknowledgment. R.A.C. thanks the National Science Foundation (Grant CHE 8820268) and the Robert A. Welch Foundation (Grant AT-532) for financial support. D.J.U. thanks the Science and Engineering Research Council for a research studentship. The advice and assistance of L. A. Melton and J. E. Elbert are gratefully acknowledged.

(31) Saltiel, J.; Khalil, G.-E.; Schanze, K. *Chem. Phys. Lett.* **1980**, *70*, 233.

L-Edge X-ray Absorption Spectroscopy of *Pyrococcus furiosus* Rubredoxin

S. J. George,[†] J. van Elp,[‡] J. Chen,[‡] Y. Ma,[§] C. T. Chen,[§] J.-B. Park,[∥] M. W. W. Adams,[∥] B. G. Searle,[⊥] F. M. F. de Groot,[#] J. C. Fuggle,[#] and S. P. Cramer*[,†,‡]

Department of Applied Science University of California Davis, California 95616 Energy and Environment Division Lawrence Berkeley Laboratory Berkeley, California 94720 AT&T Bell Laboratories Murray Hill, New Jersey 07974 Department of Biochemistry University of Georgia Athens, Georgia 30602 Department of Applied and Solid State Physics Materials Science Center, University of Groningen Nijenborgh 4, 9747 AG Groningen, The Netherlands Research Institute for Materials University of Nijmegen Toernooiveld, 6525 ED Nijmegen, The Netherlands

Received January 31, 1992

In this communication we present new experiments and theoretical simulations, using iron L-edge X-ray absorption spectroscopy, to study the metalloprotein *Pyrococcus furiosus* rubredoxin. The 3d transition metal L-edges are found between 400 and 1100 eV, in the soft X-ray region. Synchrotron radiation beam lines producing the high photon flux and high-energy resolution necessary to observe and resolve 3d transition metal L-edge spectra have only become available in the last few years.[1] L-edge spectra are interesting not only because of the 3–4-fold-higher energy resolution (vs K-edges) but also for the sensitivity to spin state, oxidation state, and ligand field offered by p → d transitions.[2-6]

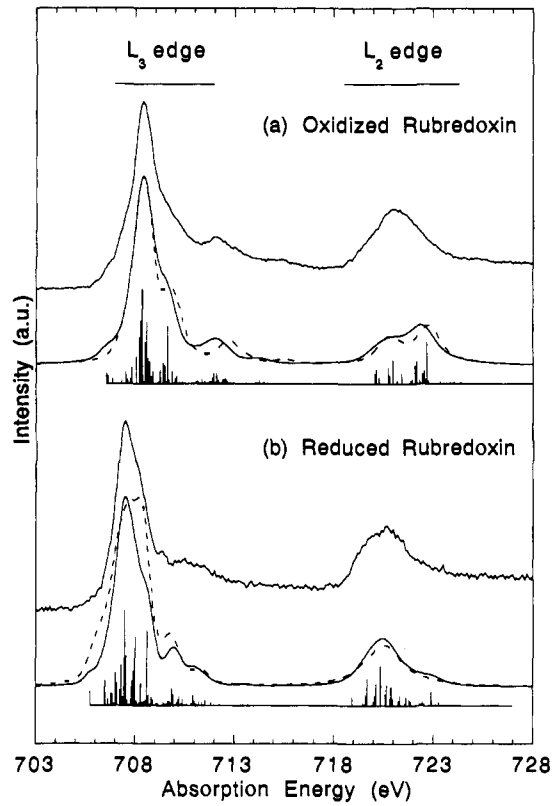

Figure 1. Experimental spectra (upper), calculated spectra (center) with (—) and without (- - -) crystal field and Slater integral reduction, and stick diagrams (lower) for the $L_{2,3}$ edges of *Pyrococcus furiosus* rubredoxin: (a) oxidized Fe^{3+} protein; (b) reduced Fe^{2+} protein. The stick diagrams show the strengths of individual transitions before line-width broadening. Indicated are the L_3 and L_2 regions of the spectrum.

In addition, the X-ray magnetic circular dichroism (XMCD) of transition metal L-edges is predicted to be strong,[7-10] and experiments have confirmed these predictions.[11]

Rubredoxins are small proteins which contain single iron atoms coordinated by a distorted tetrahedron of cysteinyl sulfur ligands.[12] This being the simplest iron–sulfur protein, an understanding of the rubredoxin electronic structure and redox mechanism is necessary for progress on biological electron transfer and more complex iron–sulfur proteins. Comparison of our experimental data with theoretical simulations reveals, as expected, an approximately tetrahedral symmetry for the Fe site. The analysis also finds similar covalency for the oxidized and reduced rubredoxin sites. Transition metal L-edge spectroscopy thus seems to be a promising new technique for bioinorganic systems.

In order to obtain the spectra, several difficulties in measuring soft X-ray absorption of metalloproteins were overcome. Because absorption cross sections in the soft X-ray region are very high,[13] work in this region requires ultrathin windows or vacuum conditions. By using partially dehydrated thin film samples,[14] 10 K

[†] University of California.
[‡] Lawrence Berkeley Laboratory.
[§] AT&T Bell Laboratories.
[∥] University of Georgia.
[⊥] University of Groningen.
[#] University of Nijmegen.

(1) Chen, C. T.; Sette, F. *Rev. Sci. Instrum.* **1989**, *60*, 1616–1621.
(2) Cramer, S. P.; de Groot, F. M. F.; Ma, Y.; Chen, C. T.; Sette, F.; Kipke, C. A.; Eichhorn, D. M.; Chan, M. K.; Armstrong, W. H.; Libby, E.; Christou, G.; Brooker, S.; McKee, V.; Mullins, O. C.; Fuggle, J. C. *J. Am. Chem. Soc.* **1991**, *113*, 7937–7940.
(3) van der Laan, G.; Zaanen, J.; Sawatzky, G. A.; Karnatak, R.; Esteva, J.-M. *Phys. Rev. B* **1986**, *33*, 4253–4263.
(4) Abbate, M.; de Groot, F. M. F.; Fuggle, J. C.; Fujimori, A.; Tokura, Y.; Fujishima, Y.; Strebel, O.; Domke, M.; Kaindl, G.; van Elp, J.; Thole, B. T.; Sawatzky, G. A.; Sacchi, M.; Tsuda, N. *Phys. Rev. B* **1991**, *44*, 5419–5422.
(5) van Elp, J.; Searle, B. G.; Sawatzky, G. A.; Sacchi, M. *Solid State Commun.* **1991**, *80*, 67–71.
(6) de Groot, F. M. F.; Fuggle, J. C.; Thole, B. T.; Sawatzky, G. A. *Phys. Rev. B* **1990**, *42*, 5459–5468.
(7) Thole, B. T.; van der Laan, G.; Sawatzky, G. A. *Phys. Rev. Lett.* **1985**, *55*, 2086–2088.
(8) Jo, T.; Sawatzky, G. A. *Phys. Rev. B* **1991**, *43*, 8771–8774.
(9) van der Laan, G.; Thole, B. T. *Phys. Rev. B* **1990**, *42*, 6670–6674.
(10) van der Laan, G.; Thole, B. T. *Phys. Rev. B* **1991**, *43*, 13401–13411.
(11) Chen, C. T.; Sette, F.; Ma, Y.; Modesti, S. *Phys. Rev. B* **1990**, *42*, 7262–7265.
(12) *Iron Sulfur Proteins*; Spiro, T. G., Ed.; Wiley-Interscience: New York, 1982.
(13) The absorption coefficient for water at the Fe L-edge is $\sim 10^4$ cm^{-1}.
(14) *Pyrococcus furiosus* rubredoxin was purified using published procedures.[15] For L-edge spectroscopy, the protein samples were partially dehydrated thin films. These were made by placing about 0.1 mL of 5.00 mM protein in 10 mM Tris·HCl buffer pH 8.0 on a silicon plate at 4 °C and evaporating under partial vacuum. The reduced rubredoxin samples contained 20 mM sodium dithionite. UV–visible absorption and EPR spectroscopy of the oxidized rubredoxin films gave spectra that were essentially identical to those of solution samples. Redissolving the films in buffer gave spectra indistinguishable from the originals by absorption and EPR spectroscopies.

0002-7863/92/1514-4426$03.00/0

temperatures, and rapid pumping, we achieved 10^{-9} mbar. This allowed windowless operation between the storage ring, sample, and detector. Low temperature data collection also helped minimize radiation damage. For detection in this region, the most commonly used method is total electron yield, in which the emission of secondary photoelectrons is measured. The ~100 Å surface sensitivity and lack of specificity make this technique impractical for large molecules dilute in metal atoms such as metalloproteins. With a seven-element soft X-ray fluorescence array detector,[17] we electronically resolved the Fe L fluorescence (705 eV) from the oxygen (525 eV), nitrogen (392 eV) and the carbon (277 eV) K fluorescence background. Since only a small fraction of absorption is due to Fe, fluorescence detection improves both the signal-to-noise and base-line stability.

L-edge data for oxidized (Fe^{3+}) and reduced (Fe^{2+}) rubredoxin are shown in Figure 1,[16] together with results of theoretical calculations. The reduced L_3 edge has a maximum near 707.5 eV, a higher energy shoulder, and diffuse absorption features extending to 713 eV. The L_2 edge is broader and also tails to higher energy. Upon oxidation of the protein there is a ~800 meV increase in the main peak position, and the higher energy features become better separated.

To interpret these spectra, we used a theoretical simulation approach developed by Sawatzky, Thole, Fuggle, deGroot, and co-workers,[6,18,19] based on earlier work by Cowan[20] and Butler.[21] The calculation[22] describes the transition from $3d^5$ (Fe^{3+}) and $3d^6$ (Fe^{2+}) to $\underline{2p}3d^6$ and $\underline{2p}3d^7$ (where $\underline{2p}$ stands for the 2p core hole) in tetrahedral symmetry. The detailed structure at the L_3 ($2p_{3/2}$) and L_2 ($2p_{1/2}$) edges arises from final-state multiplet splittings from 3d–3d and 2p–3d Coulomb and exchange interactions, as well as ligand field d-orbital splittings. For simulating covalency effects on the experimental spectra, separation of the multiplet features can be controlled by an empirical reduction in the Slater integrals. Even for relatively ionic systems, electron correlation effects commonly require Slater integral reductions to 80% of theoretical values. In the rubredoxin simulations, the covalency of the S ligands is reflected in additional reductions (to ~70%) required to model the data. Surprisingly, the covalency determined from the Slater integral reduction is similar for reduced and oxidized rubredoxin. Although one might expect that upon oxidation the extra hole would be mainly localized on the S neighbors, increasing the covalency, this might be counteracted by strong exchange stabilization of the high-spin $3d^5$ state.

Adjusting $10Dq$ in the simulations changes the spectral splittings and intensities, especially for the low-energy features below the strongest L_3 peak. The differences between purely atomic and ligand field calculations are illustrated in Figure 1. We found that $10Dq$ values of -0.75 ± 0.1 eV for Fe^{3+} and -0.60 ± 0.1 eV for Fe^{2+} gave reasonable simulations. Despite considerable optical work,[23-26] $10Dq$ values for rubredoxin have not been reported. The X-ray parameters are similar to optical values for rubredoxin analogues $Fe^{III}[S(2,3,5,6\text{-}Me_4C_6H)]_4^-$ ($10Dq = -0.55$ eV)[26] and $Fe^{II}[S(2\text{-}PhC_6H_4)]_4^{2-}$ ($10Dq = -0.43$ eV).[27] Some caution must be used in comparing $10Dq$ values, because the XAS $10Dq$ value is determined by the $\underline{2p}3d^{n+1}$ final states instead of the $3d^n$ multiplet states.

Certain discrepancies remain. There is additional intensity at the high-energy side of the L_3 edge (~712 eV): for Ni compounds this was shown to be a satellite structure.[3] Although the experimental oxidized rubredoxin L_2 edge is broad and symmetric, the simulations gave an asymmetric double-peaked structure. Calculations assuming D_{2d} symmetry did not significantly improve the modeling. Although additional work is needed to fully explain the spectra, soft X-ray spectroscopy can be a valuable tool for bioinorganic studies.

Acknowledgment. This work was supported by the National Institutes of Health, Grant GM-44380 (to S.P.C.), and by LBL Exploratory Research Funds (to S.P.C.). National Science Foundation Grant DMB-88-05-255 (to M.W.W.A.) and support from the Netherlands Foundation for Chemical Research and the Committee for European Development of Science and Technology (to B.G.S.) are acknowledged. The National Synchrotron Light Source is funded by the Department of Energy, Office of Basic Energy Sciences.

(15) Blake, P. R.; Park, J.-B.; Bryant, F. O.; Aono, S.; Magnuson, J. K.; Eccleston, E.; Howard, J. B.; Summers, M. F.; Adams, M. W. W. *Biochemistry* **1991**, *30*, 10885–10895.

(16) The L-edge spectra were measured using AT&T Bell labs beam line U-4B[1] at the National Synchrotron Light Source, Brookhaven National Laboratory. A refocusing mirror produced a focused beam spot (1 mm × 1.5 mm) enabling the sample to be mounted at glancing incidence (around 15° with respect to the incoming beam) without loss of incident X-ray intensity. Fluorescent X-rays from the protein samples were detected using a specially designed windowless seven-element germanium detector.[17] The chamber was maintained at a vacuum of 2×10^{-9} mbar or better. After equilibration in a loadlock to 10^{-5} mbar, the samples were introduced into the main chamber and mounted on a precooled 10 K cold finger attached to a liquid helium flow cryostat. The L-edge spectra were collected as repetitive ~15-min scans over a few hours. They were calibrated using the peak positions of the total electron yield spectra of MnF_2 and NiF_2, with absorption maxima assigned as 640.0 and 852.7 eV, respectively.

(17) Cramer, S. P.; Tench, O.; Yocum, M.; Kraner, H.; Rogers, L.; Radeka, V.; Mullins, O.; Rescia, S. *X-ray absorption fine structure—Proceedings of the 6th International XAFS Conference*; Hasnain, S. S., Ed.; Ellis Horwood: Chichester, 1991; pp 640–645.

(18) Thole, B. T.; Cowan, R. D.; Sawatzky, G. A.; Fink, J.; Fuggle, J. C. *Phys. Rev. B* **1985**, *31*, 6856–6858.

(19) de Groot, F. M. F.; Fuggle, J. C.; Thole, B. T.; Sawatzky, G. A. *Phys. Rev. B* **1990**, *41*, 928–937.

(20) Cowan, R. D. *The Theory of Atomic Structure and Spectra*; University of California Press: Berkeley, 1981.

(21) Butler, P. H. *Point Group Symmetry, Applications, Methods, and Tables*; Plenum: New York, 1981.

(22) We used reduced Slater integrals F^2_{dd} and F^4_{dd} at 65% (d–d) and F^2_{pd}, G^1_{pd}, and G^3_{pd} at 72.5% (p–d) for Fe^{3+} and 65% (all) for Fe^{2+}. To describe the different broadening processes present we broadened the spectra with a Lorentzian of 0.5 eV (L_3) and 1.0 eV (L_2) for the Fe^{3+} and 0.2 eV (L_3) and 0.8 eV (L_2) for the Fe^{2+} and convoluted with a Gaussian of 0.3 eV (Fe^{3+}) and 0.25 eV (Fe^{2+}).

(23) Bertrand, P.; Gayda, J.-P. *Biochim. Biophys. Acta* **1988**, *954*, 347–350.

(24) Bennett, D. E.; Johnson, M. K. *Biochim. Biophys. Acta* **1987**, *911*, 71–80.

(25) Eaton, W. A.; Lovenberg, W. In *Iron–Sulfur Proteins*; Academic Press: New York, 1973; Vol. II, pp 131–162.

(26) Gebhard, S. M.; Deaton, J. S.; Koch, S. A.; Millar, M.; Solomon, E. I. *J. Am. Chem. Soc.* **1990**, *112*, 2217–2231.

(27) Gebhard, S. M.; Koch, S. A.; Millar, M.; Devlin, F. J.; Stephens, P. J.; Solomon, E. I. *J. Am. Chem. Soc.* **1991**, *113*, 1640–1649.

Electrophilic Reactions of Protonated *closo*-$B_{10}H_{10}^{2-}$ with Arenes, Alkane C–H Bonds, and Triflate Ion Forming Aryl, Alkyl, and Triflate *nido*-6-X-$B_{10}H_{13}$ Derivatives

M. Frederick Hawthorne,* Ipe J. Mavunkal, and Carolyn B. Knobler

Department of Chemistry and Biochemistry
University of California at Los Angeles
Los Angeles, California 90024

Received February 21, 1992

The preferred synthesis of *closo*-$B_{10}H_{10}^{2-}$ utilizes the loss of two skeletal electron pairs and two protons from *arachno*-6,9-$B_{10}H_{12}L_2$ where L = two-electron donor (eq 1).[1] The reverse process was later reported using HCl as the proton source and typically $(C_2H_5)_2S$ as the electron donor.[2]

$$\textit{arachno}\text{-}6,9\text{-}B_{10}H_{12}L_2 \rightleftharpoons \textit{closo}\text{-}B_{10}H_{10}^{2-} + 2L: + 2H^+ \quad (1)$$

We now report the facile two-electron reduction of *closo*-$B_{10}H_{10}^{2-}$ by reaction with benzene, cyclohexane, or triflate ion in the presence of triflic acid (CF_3SO_3H) forming the corre-

(1) (a) Hawthorne, M. F.; Pitochelli, A. R. *J. Am. Chem. Soc.* **1959**, *81*, 5519. (b) *Inorganic Syntheses*; Tyree, S. Y., Ed.; McGraw-Hill: New York, 1967; Vol. 9, p 16.

(2) Marshall, M. D.; Hunt, R. M.; Hefferman, G. T.; Adams, R. M.; Makhlouf, J. M. *J. Am. Chem. Soc.* **1967**, *89*, 3361.

0002-7863/92/1514-4427$03.00/0